Am J Physiol Renal Physiol 295: F1472–F1484, 2008.
First published September 3, 2008; doi:10.1152/ajprenal.90229.2008.

WNK3 positively regulates epithelial calcium channels TRPV5 and TRPV6 via a kinase-dependent pathway

Wei Zhang, Tao Na, and Ji-Bin Peng

Nephrology Research and Training Center, Division of Nephrology, Department of Medicine, University of Alabama at Birmingham, Birmingham, Alabama

Submitted 1 April 2008; accepted in final form 28 August 2008

Zhang W, Na T, Peng J-B. WNK3 positively regulates epithelial calcium channels TRPV5 and TRPV6 via a kinase-dependent pathway. *Am J Physiol Renal Physiol* 295: F1472–F1484, 2008. First published September 3, 2008; doi:10.1152/ajprenal.90229.2008.—WNK3, a member of the With No Lysine (K) family of protein serine/threonine kinases, was shown to regulate members of the SLC12A family of cation-chloride cotransporters and the renal outer medullary K^+ channel ROMK and Cl^- channel SLC26A9. To evaluate the effect of WNK3 on TRPV5, a renal epithelial Ca^{2+} channel that serves as a gatekeeper for active Ca^{2+} reabsorption, WNK3 and TRPV5 were coexpressed in *Xenopus laevis* oocytes and the function and expression of TRPV5 were subsequently examined. An 82.7 ± 7.1% increase in TRPV5-mediated Ca^{2+} uptake was observed when WNK3 was coexpressed. A similar increase in TRPV5-mediated Na^+ current was observed with the voltage-clamp technique. WNK3 also enhanced Ca^{2+} influx and Na^+ current mediated by TRPV6, which is the closest homolog of TRPV5 that mediates active intestinal Ca^{2+} absorption. The kinase domain of WNK3 alone was sufficient to increase TRPV5-mediated Ca^{2+} transport, and the positive regulatory effect was abolished by the kinase-inactive D294A mutation in WNK3, indicating a kinase-dependent mechanism. The complexly glycosylated TRPV5 that appears at the plasma membrane was increased by WNK3. The exocytosis of TRPV5 was increased by WNK3, and the effect of WNK3 on TRPV5 was abolished by the microtubule inhibitor colchicine. The increased plasma membrane expression of TRPV5 was likely due to the enhanced delivery of mature TRPV5 to the plasma membrane from its intracellular pool via the secretory pathway. These results indicate that WNK3 is a positive regulator of the transcellular Ca^{2+} transport pathway.

calcium absorption; reabsorption; WNK4

WNKS [With No lysine (K)] kinases, which form a unique protein kinase subfamily in the kinome, are characterized by the cysteine substitution of a highly conserved lysine residue in the catalytic domain (39, 63). The four WNK kinases share a common structural feature of the conserved serine-threonine kinase domain in the NH_2-terminal region, an autoinhibitory domain following the kinase domain, a short acidic domain, and two putative coiled-coil domains in the COOH-terminal region (56, 60). The physiological significance of WNK kinases was demonstrated by the association of mutations in the *WNK1* or *WNK4* gene and a genetic form of hypertension, known as familial hyperkalemic hypertension (FHH), or pseudohypoaldosteronism type II (PHAII), or Gordon's syndrome (60). Deletions in the first intron of the *WNK1* gene, which result in an increased expression of WNK1, or point mutations in the acidic motif of WNK4, all lead to FHH (60). While clinical manifestations such as hyperkalemia, hypertension, mild metabolic acidosis, low renin, and normal glomerular filtration rate are commonly present in FHH (23), patients with Q565E mutation in WNK4 also exhibit hypercalciuria and hypersensitivity to thiazide diuretics (37, 38), whereas patients with WNK1 mutation do not show urinary calcium wasting (1).

The nature of electrolyte imbalance in FHH motivated the studies on the effects of WNKs on ion transport proteins. WNK4 was shown to inhibit the thiazide-sensitive Na-Cl cotransporter (NCC) (5, 21, 22, 61, 67–69) and other members of the SLC12A family (20, 28), the renal outer medullary K^+ channel (ROMK) (24, 31, 50), the epithelial sodium channel (ENaC) (16, 49, 50), and osmolarity-sensitive calcium-permeable channel TRPV4 (17), and to enhance epithelial calcium channel TRPV5 (27). WNK1, on the other hand, regulates ENaC (41, 64, 65) and ROMK (11, 33, 59) in a manner independent of its kinase activity. In addition, WNK4 and WNK1 also regulate paracellular Cl^- permeability through regulating the claudins (29, 42, 66). Both WNK1 and WNK4 can also regulate SLC12A members through the activation of STE20 kinases (2, 18, 40, 57, 58). Misregulation of NCC by WNK4 mutants was confirmed in transgenic mouse studies and is most relevant to the pathogenesis of FHH (32, 70). WNK3 has been shown to be a potent regulator of the SLC12A family of electroneutral cation/Cl^- cotransporters in a kinase-dependent manner (12, 30, 47, 48). In contrast to the effects of WNK3 on SLC12A family members, WNK3 decreases the plasma membrane expression of ROMK1 independent of its kinase activity (34). Similarly, the Cl^- channel SLC26A9 is also inhibited by WNK3 in a kinase-independent manner (14).

TRPV5 and TRPV6 are Ca^{2+}-selective channels, which mediated the apical Ca^{2+} entry process of the transcellular calcium transport pathway in the kidney and intestine, respectively (25, 45). TRPV5 knockout mice exhibit a 6- to 10-fold increase in urinary Ca^{2+} excretion (26); and TRPV6 knockout mice show a 60% reduction in intestinal and a 40% reduction in placental calcium transport (3, 52). To keep up with the body's need for Ca^{2+}, TRPV5/6-mediated Ca^{2+} transport is under vigorous regulation. TRPV5 and TRPV6 are regulated at mRNA level by hormones, such as 1,25-dihydroxyvitamin D_3 (51, 53, 62) and estrogen (54). In addition, the trafficking and stability of TRPV5 and TRPV6 proteins are regulated by proteins such as S100A10-annexin II complex (55) and β-glucuronidase Klotho, respectively (7, 9). Protein kinases are also involved in the regulation of TRPV5 and TRPV6. PKC was shown to regulate TRPV5 (8), and the serum and glucocorti-

Address for reprint requests and other correspondence: J.-B. Peng, Univ. of Alabama at Birmingham, Div. of Nephrology, ZRB 625, 1900 University Blvd., Birmingham, AL 35294-0006 (e-mail: jpeng@uab.edu).

The costs of publication of this article were defrayed in part by the payment of page charges. The article must therefore be hereby marked "*advertisement*" in accordance with 18 U.S.C. Section 1734 solely to indicate this fact.

coid inducible kinases SGK1 and SGK3 were reported to regulate both TRPV5 and TRPV6 (4, 15). Because patients carrying the Q565E mutation of WNK4 exhibit hypercalciuria, we recently studied the effect of WNK4 on TRPV5 (27). WNK4 enhances TRPV5-mediated Ca^{2+} transport by increasing its membrane expression without a corresponding effect on TRPV6. In fact, TRPV5 is the only ion transport protein in the transcellular ion transport pathways that is upregulated by WNK4. In contrast, TRPV4, a closely related member of the TRP family, is inhibited by WNK4 (17). The mechanism underlying the opposite effects of WNK4 on TRPV5 and other ion transport protein is unclear. Interestingly, WNK3 positively regulates NCC, in striking contrast to the inhibitory effect of WNK4 (48, 68). This motivated us to investigate whether the antagonistic effects of WNK3 and WNK4 are preserved on TRPV5 as well. WNK3 is expressed in the distal convoluted tubule (DCT), where TRPV5 is coexpressed (48), and also in extrarenal tissues such as intestine, stomach, epididymis, and pancreas (30) where TRPV6 is expressed (45, 46, 71). Thus WNK3 could be a physiological regulator of both TRPV5 and TRPV6.

In this study, we showed that WNK3 is capable of stimulating not only TRPV5 but also TRPV6. We also demonstrated that the kinase domain of WNK3 is necessary and sufficient to mediate this regulation, which involves protein maturation and delivery to the plasma membrane via the secretory pathway.

MATERIALS AND METHODS

cDNA constructs. Human TRPV5 and TRPV6 cDNAs were described previously (44). Human WNK4 cDNA was generously provided by Drs. Xavier Jeunemaitre and Juliette Hadchouel. Full-length human WNK3 cDNA was purchased from OriGene (Rockville, MD). Mouse NCC cDNA (IMAGE:4237274, GenBank accession no. BC038612) was purchased from Open Biosystems (Huntsville, AL). The cDNAs were subcloned into the *Xenopus laevis* oocytes expression vector pIN (27). For visualizing TRPV5 in *X. laevis* oocytes, a yellow fluorescent protein (YFP) was incorporated into the COOH terminus of TRPV5 (TRPV5-YFP). To detect TRPV5 proteins expressed at the cell surface, a hemaglutinin epitope (HA tag) with double glycines GGYPYDVPDYA was inserted into the first extracellular loop of human TRPV5 between arginine 355 and glycine 356, using a PCR-based approach. WNK3 D294A and Q545E mutants and TRPV5 N358Q and S556C mutants were generated using a QuikChange II site-directed mutagenesis kit (Stratagene, La Jolla, CA) following the manufacturer's instruction. All the mutants were confirmed by sequencing.

Ca^{2+} uptake in X. laevis oocytes. In vitro transcription, injection of the resultant capped synthetic complementary RNAs (cRNAs) into oocytes, and $^{45}Ca^{2+}$ uptake assay in oocytes were conducted as described previously (45). The animal protocol used in this study was approved by the Institutional Animal Care and Use Committee of the University of Alabama at Birmingham. cRNAs were injected at 12.5 ng/oocyte. When a combination of two or three cRNAs was required, we mixed the cRNAs in a way that the concentration of individual

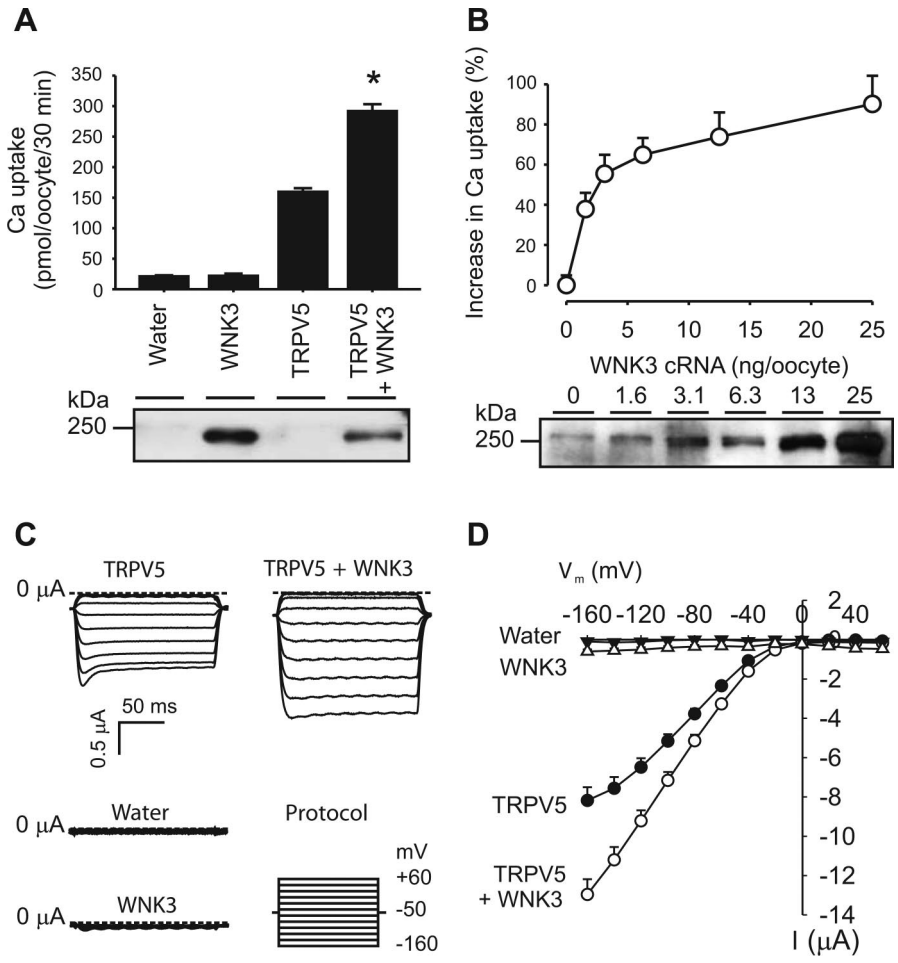

Fig. 1. With No Lysine (K) 3(WNK3) increased the renal epithelial calcium channel (TRPV5)-mediated Ca^{2+} uptake and Na^+ current. *A*: TRPV5-mediated $^{45}Ca^{2+}$ uptake was increased when TRPV5 and WNK3 were coexpressed in *Xenopus laevis* oocytes. Data are presented as means ± SE of 8 independent experiments. *$P < 0.01$ vs. TRPV5 alone group. *Bottom*: representative Western blot analysis using an antibody against WNK3, showing the expression of WNK3 in respective groups. *B*: WNK3 increased TRPV5-mediated $^{45}Ca^{2+}$ uptake dose dependently. Groups of *X. laevis* oocytes were injected with 12.5 ng TRPV5 cRNA with 0, 1.6, 3.1, 6.3, 13, or 25 ng WNK3 cRNA and $^{45}Ca^{2+}$ uptake experiments were performed 2 days later. Data from 3 independent experiments are presented as percentage of increase over the group of oocytes injected with TRPV5 cRNA alone. A representative Western blot analysis (*bottom*) shows the level of WNK3 proteins in each group. A band slightly higher than that of exogenous WNK3 was detected in the oocytes not injected with WNK3 cRNA. *C*: representative traces of Na^+ current in the absence of extracellular Ca^{2+} for TRPV5 in the presence and absence of WNK3. Na^+-evoked currents were obtained by subtracting currents recorded in the choline solution (0 mM Na^+) from those recorded in Na^+ solution (100 mM Na^+). Water-injected control oocytes (Water) and WNK3-injected oocytes exhibited negligible currents. *D*: current-voltage (*I-V*) plots of Na^+-evoked currents in water-injected control oocytes (Water) or oocytes expressing WNK3, TRPV5, or both TRPV5 and WNK3. Data are expressed as means ± SE of 22–32 oocytes in each group from 4 independent experiments. All experiments were performed at 2 days after injection of cRNAs.

cRNA was maintained. Defolliculated *X. laevis* oocytes were kept at 18°C in 0.5× L15 medium (Invitrogen, Carlsbad, CA) supplemented with 10 mM HEPES (pH 7.6), 5% heat-inactivated horse serum, penicillin at 10,000 units/l, streptomycin at 10 mg/l, and amphotericin B at 25 μg/l. Two days after injection, uptake experiments were carried out at room temperature (24°C) for a period of 30 min. Standard uptake solution contained (in mM) 100 NaCl, 2 KCl, 1 $MgCl_2$, 1 $CaCl_2$ (including $^{45}CaCl_2$ at 10 μCi/ml), and 10 HEPES, pH 7.5. After uptake, oocytes were washed six times with ice-cold standard uptake solution without $^{45}CaCl_2$, and then they were dissolved in 10% SDS. The incorporated $^{45}Ca^{2+}$ was determined using a scintillation counter. Ca^{2+} uptake data are presented as mean values from at least three experiments with seven to nine oocytes per group, using SE as the index of dispersion.

Two-microelectrode voltage clamp. The two-microelectrode voltage-clamp experiments were performed as described previously (27, 45) with a GeneClamp 500 amplifier and pCLAMP software (version 9, Axon Instruments, Foster City, CA). The resistance of microelectrodes filled with 3 M KCl was 0.5–2 MΩ. In experiments involving voltage jumps, the oocyte was clamped at the holding potential of −50 mV. Voltage pulses (100 ms) between −160 and +60 mV, in increments of 20 mV, were then applied, and steady-state currents were obtained as the average values in the interval from 60 to 95 ms after the initiation of the voltage pulses. The standard perfusion solution used contained (in mM) 100 choline-Cl, 2 KCl, 1 $MgCl_2$, and 10 HEPES, pH 7.5 (adjusted using Tris base and HCl). Choline-Cl was substituted with NaCl when the Na^+ current was tested.

Surface expression measurement. Surface expression of TRPV5 tagged with HA in the extracellular loop was assessed based on the approach described by Palmada et al. (43). Water-injected oocytes and oocytes injected with cRNA for HA-TRPV5 alone or with WNK3 were incubated at 18°C for 2 days. The oocytes were then blocked for 60 min in modified Barth's solution with 1% BSA at 4°C, labeled with mouse monoclonal anti-HA antibody (H-9658, 1:50,000, Sigma-Aldrich) in 1% BSA for 60 min at 4°C, washed at 4°C (30 min ×2), and incubated with horseradish peroxidase (HRP)-coupled secondary antibody (sc-2064, goat anti-mouse, 1:25,000, Santa Cruz Biotechnology, Santa Cruz, CA), in 1% BSA for 60 min. Oocytes were extensively washed (modified Barth's solution without BSA, 4°C, 10 min ×12). Individual oocytes were placed in 25 μl SuperSignal ELISA Femto Maximum Sensitivity Substrate (Pierce Biotechnology, Rockford, IL) and incubated at room temperature for 1 min. Chemiluminescence was quantified using a FB12-single tube luminometer (Berthold Detection Systems, Pforzheim, Germany) and recorded by FB12/Sirius Software.

Western blot analysis and surface biotinylation. Two days after injection with different cRNAs, oocytes were washed with modified Barth's solution. Oocytes were lysed with lysis buffer (100 mM NaCl, 20 mM Tris·Cl, 1% Triton X-100 plus protease inhibitor cocktail, pH 7.6) at 20 μl/oocyte and centrifuged at 5,000 rpm for 10 min at 4°C to remove the cellular debris and yolk proteins. Cell lysates were subjected to SDS-PAGE. In general, the extract supernatant corresponding to one oocyte was loaded per lane. After SDS-PAGE, the proteins were transferred to polyvinylidene difluoride membranes. Membranes were blocked with PBS containing 0.5% Tween 20 and 5% nonfat milk for 1 h at room temperature. Primary antibody was incubated overnight at 4°C, followed by multiple washes in PBS-Tween 20. TRPV5 (1:3,000 dilution) and WNK3 (1:1,500 dilution)

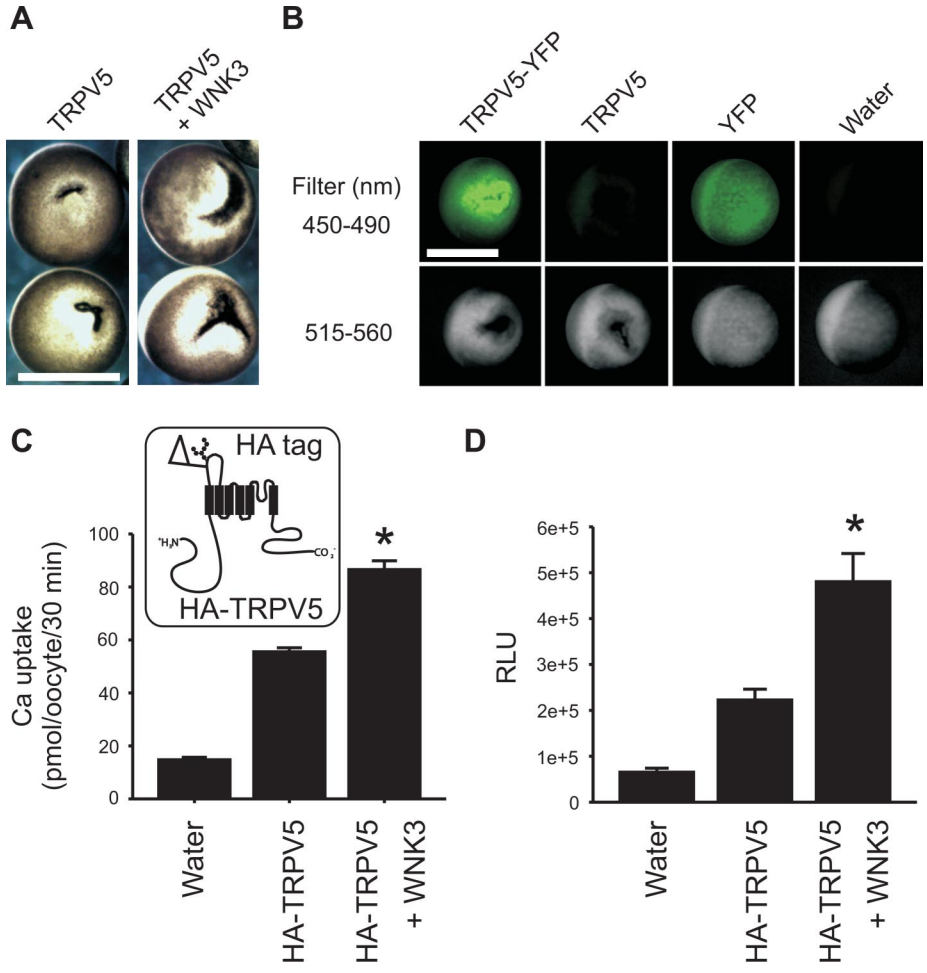

Fig. 2. WNK3 increased TRPV5 expression at the oocyte surface. *A*: size of scarlike mark in TRPV5-expressing oocytes was increased by WNK3 compared with the oocytes expressing TRPV5 alone 18 h after cRNA injection. No scars were observed in control oocytes or oocytes expressing WNK3 or WNK4 alone. Bar = 1 mm. *B*: scarlike mark correlated with TRPV5 expression. A control water-injected oocyte (water) or an oocyte expressing TRPV5 tagged with yellow fluorescent (TRPV5-YFP), TRPV5, or YFP was imaged with a fluorescence microscope first under the FITC filter (450–490 nm; *top* row) and subsequently under the rhodamine filter (515–560 nm; *bottom* row). A scarlike mark was visible in the oocyte expressing TRPV5-YFP or TRPV5, but not in the oocyte expressing YFP or in the control oocyte. A high level of fluorescence was observed in the mark area in the oocyte expressing TRPV5-YFP. Bar = 1 mm. *C*: TRPV5 construct with hemaglutinin (HA) epitope in the first extracellular loop (HA-TRPV5, model shown in *inset*) was capable of mediating $^{45}Ca^{2+}$ uptake and was responsive to WNK3. *D*: surface level of HA-TRPV5 was increased in the presence of WNK3. The control water-injected oocytes (Water) and the oocytes expressing HA-TRPV5 alone or with WNK3 were probed first with a mouse monoclonal antibody against HA and then a HRP-coupled secondary antibody. Chemiluminescence signal of individual oocytes developed with HRP substrate was detected with a luminometer. Data from 24 to 40 oocytes in each group from two batches of oocytes are presented as means ± SE. *$P < 0.01$ vs. HA-TRPV5 alone group.

antibodies were purchased from Alpha Diagnostic International (San Antonio, TX), and TRPV6 antibody (sc-31445, 1:3,000 dilution) was purchased from Santa Cruz Biotechnology. The appropriate HRP-conjugated secondary antibodies (1:3,000 dilution, Pierce Biotechnology) were incubated in the blocking solution for 1 h at room temperature, followed by multiple washes with PBS-Tween 20. Chemiluminescence was detected using a SuperSignal West Femto Maximum Sensitivity Substrate kit (Pierce) in accordance with the manufacturer's protocol. Relative amounts of each band were quantified using an Epson Perfection V200 scanner (Epson, Long Beach, CA) and Gel-Pro Analyzer 4.0 (Media Cybernetics, Silver Spring, MD). Biotinylation experiments were performed as described previously using Sulfo-NHS-SS-Biotin (Pierce Biotechnology) (27).

Oocyte imaging, volume, and surface measurement. To measure oocyte surface area or volume, images of oocytes were captured with a DCM500 digital camera for a microscope (ScopePhoto, Madell Technology, Beijing, China) 2 days after injection of oocytes with different cRNAs. Diameters of oocytes were measured using ScopePhoto software. Surface area and volume of oocytes were respectively calculated using the equations $A = 4\pi r^2$ and $V = 4/3\pi r^3$, where A is the surface area, V is the volume, and r is the radius.

The fluorescent images of oocytes expressing TRPV5 tagged with yellow fluorescent protein (TRPV5-YFP), TRPV5, or YFP were captured using a Leica DC500 12 Megapixel camera and Leica DMIRB fluorescence microscope (Leica Microsystems, Heerburgg, Switzerland) first with and FITC filter (blue, 450–490 nm/LP515) and then with a rhodamine filter (green, 515–560 nm/LP590).

Rate of TRPV5 exocytosis. To examine the effect of WNK3 on TRPV5 exocytosis, we adopted an approach of measuring the rate of ENaC exocytosis in *X. laevis* oocytes (6). Oocytes were coinjected with the S556C mutant of TRPV5, with or without WNK3. A previous study showed that TRPV5 proteins with cysteine at position 556 are inhibited when oocytes are incubated with the cell-impermeable thiol reagent 2-trimethylammonium-ethyl-methanethiosulfonate bromide (MTSET; Toronto Research Chemicals, North York, Ontario, Canada) (13). The oocytes were incubated with 2 mM MTSET for 5 min, which is sufficient to irreversibly inhibit the majority of functional TRPV5 channel proteins at the oocyte surface. After incubation with MTSET, the Na^+-evoked current was measured immediately and every 2 min for a 10-min period using the voltage-clamp technique. Subsequent delivery of unmodified TRPV5 proteins from the intracellular pool to the plasma membrane results in a time-dependent increase in TRPV5-mediated Na^+ currents, which reflect the rate of TRPV5 exocytosis.

Glycosylation analysis. Lysates of *X. laevis* oocytes expressing TRPV5 were treated with peptide:*N*-glycosidase F (PNGase F) or endoglycosidase H (Endo H) following the manufacturer's instructions (New England Biolabs, Beverly, MA). An equal amount of lysates was denatured at 65°C for 10 min. After the addition of one-tenth volume of appropriate 10× reaction buffer (and 10% NP-40 for the PNGase F reaction) and 2 μl (1,000 U) of PNGase F, Endo H, or water (in control reactions), samples in 40 μl of total reaction volume were incubated at 37°C for 1–2 h. After the incubation, an equal volume of 2× sample buffer was added to each reaction. The resultant samples were then analyzed by SDS-PAGE and Western blot.

RESULTS

WNK3 increased TRPV5-mediated Ca^{2+} transport and Na^+ current. When TRPV5 was expressed in *X. laevis* oocytes, Ca^{2+} influx was significantly increased over the water-injected control group as measured by radiotracer $^{45}Ca^{2+}$ uptake assay 2 days after injection (Fig. 1*A*). Ca^{2+} influx was not significantly increased in oocytes expressing WNK3 alone; however, an 82.7 ± 7.1% increase in Ca^{2+} influx was observed in oocytes expressing both WNK3 and TRPV5 over that in oocytes expressing TRPV5 alone. The expression of exogenous WNK3 in respective groups was confirmed by Western

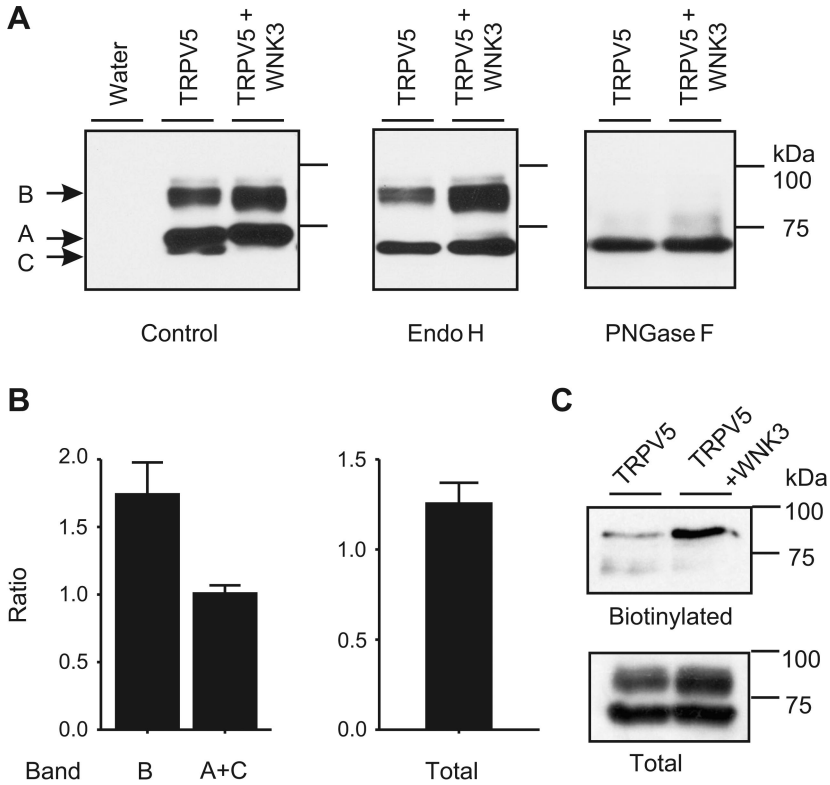

Fig. 3. WNK3 increased the complexly glycosylated form of TRPV5. *A*: level of complexly glycosylated TRPV5 (*band B*) was increased and the unglycosylated form (*band C*) was decreased in the presence of WNK3 (*left*). *Band B* increased by WNK3 was resistant to endoglycosidase H (Endo H; *middle*) but was sensitive to PNGase F (*right*). *B*: intensity ratios of *bands B*, *A*, and *C* (*left*) and all the bands combined (*right*) between the oocytes expressing TRPV5 alone and the oocytes expressing TRPV5 and WNK3. Data from 5 experiments are presented as means ± SE. *C*: level of biotinylated TRPV5 protein at the oocyte surface (*top*) was higher in oocytes expressing both TRPV5 and WNK3 than those expressing TRPV5 alone. Each lane was loaded with biotinylated proteins equal to 5 oocytes. The corresponding total TRPV5 proteins are shown (*bottom*). Each lane was loaded with proteins equal to a quarter of an oocyte. The exposure time for the biotinylated proteins was ~5 times that for the total proteins.

blot analysis with an antibody against WNK3 (Fig. 1*A*, *bottom*). The effect of WNK3 on TRPV5 was dose dependent (Fig. 1*B*). We used a saturating level of WNK3 cRNA (12.5 ng/oocyte) in the following experiments, although WNK3 exerted a significant enhancing effect on TRPV5-mediated Ca^{2+} influx at cRNA amount as low as 1.6 ng/oocyte (Fig. 1*B*).

In the absence of extracellular Ca^{2+}, Na^+ current mediated by TRPV5 was also increased by WNK3 at negative membrane potentials using the voltage-clamp technique (Fig. 1, *C* and *D*).

WNK3 increased plasma membrane expression of TRPV5. After injection with TRPV5 cRNA, a scarlike mark emerged at the cell surface around the animal pole of *X. laevis* oocytes as early as 12 h after injection (Fig. 2, *A* and *B*). The scarlike mark was likely resulting from an aggregation of pigment due to the aggregation of underneath cytoskeleton components caused by excessive Ca^{2+} influx, although the exact mechanism is yet to be determined. When TRPV5 was coexpressed with WNK3, the mark appeared earlier and the scale of the mark was also increased (Fig. 2*A*). Similar marks were not observed in oocytes expressing WNK3, WNK4, or TRPV6 (data not shown). To understand the relationship between the mark and TRPV5 expression, we tagged TRPV5 with YFP at its COOH terminus so that TRPV5-YFP protein could be visualized under the fluorescent microscope. The TRPV5-YFP cRNA-injected oocytes showed a similar scarlike mark on the oocyte surface, whereas no mark was observed in oocytes injected with YFP cRNA (Fig. 2*B*). When YFP was excited at 450–490 nm, distribution of the YFP or TRPV5-YFP in oocytes was visible. While YFP was evenly distributed in the oocytes, TRPV5-YFP was rather concentrated in a small area where the scarlike mark was situated (Fig. 2*B*). Outside the mark, the TRPV5-YFP level was much lower. Although a high level of TRPV5-YFP proteins was distributed over the scarlike mark area, the scale of the mark may not be a direct measure of TRPV5 protein level. TRPV5 is likely only one of many membrane proteins gathering over the scar area due to their association with the aggregated cytoskeleton in the animal pole. Furthermore, the scarlike mark may not be unique to the expression of TRPV5. TRPV6, whose Ca^{2+} influx value is less than half that of TRPV5, did not induce scarlike mark formation. However, mutants of TRPV6 with increased Ca^{2+} influx comparable to TRPV5 also induced a scarlike mark (Na T, Zhang W, and Peng J, unpublished observations). Thus the level of Ca^{2+} influx, not necessarily the level of protein expression, appeared key to scarlike mark formation.

To directly measure the level of TRPV5 protein at the cell surface, we inserted a HA tag in the first extracellular loop of TRPV5 (Fig. 2C, *inset*) according to the approach described by Palmada et al. (43). The HA-tagged TRPV5 (HA-TRPV5) was functional and could be increased by WNK3 to a similar extent of wild-type TRPV5 (Fig. 2*C*). We then probed the HA level at the cell surface with a mouse monoclonal anti-HA antibody. After incubation with a HRP-conjugated secondary antibody and thorough washes, the substrate of HRP was then applied to oocytes. Light emission of individual oocytes that reflects the HA-TRPV5 level was then determined using a luminometer. Consistent with the increase in Ca^{2+} uptake, the level of HA-TRPV5 signal at the cell surface doubled in the presence of WNK3 (Fig. 2*D*).

WNK3 increased forward trafficking of TRPV5 via the secretory pathway. To further understand the nature of the effect of WNK3 on TRPV5, we next examined which form of TRPV5 was altered by WNK3. TRPV5 proteins migrate in three major bands in SDS-PAGE: *band A* represents core-glycosylated form, *band B* represents the complexly glycosylated form, and *band C* is the unglycosylated band. Only the complexly glycosylated form (*band B*) is expressed in the plasma membrane (27). In the presence of exogenous WNK3, there was a decrease in the level of the unglycosylated form (*band C*), and an increase in the complexly glycosylated form (*band B*) (Fig. 3*A*, *left*). The increase in the complexly glycosylated TRPV5 became more apparent after digestion with Endo H, which cleaves within the chitobiose core of high mannose and some hybrid oligosaccharides from *N*-linked glycoproteins (36) (Fig. 3*A*, *middle*). In contrast, after the removal of all the *N*-linked oligosaccharides by PNGase F, the total level of TRPV5 protein appeared to be not as different as the complexly glycosylated form of TRPV5 (*band B*) between the TRPV5 alone group and the group coexpressed with WNK3 (Fig. 3*A*, *right*). Based on the band intensities of five independent experiments, a 74.1 ± 23.7% increase by WNK3 was observed for *band B*, no increase was observed for *bands A* and *C* combined (0.8 ± 6.1%) (Fig. 3*B*, *left*). When all the bands were combined, a 25.5 ± 11.6% increase of total TRPV5 protein by WNK3 was evident (Fig. 3*B*, *right*). The increase in surface expression of TRPV5 was further confirmed by biotinylation studies (Fig. 3*C*).

N-linked glycoproteins are core-glycosylated in the endoplasmic reticulum and oligosaccharides are further processed in the Golgi apparatus and along the *trans*-Golgi network. After complexly glycosylated along the secretory pathway, the

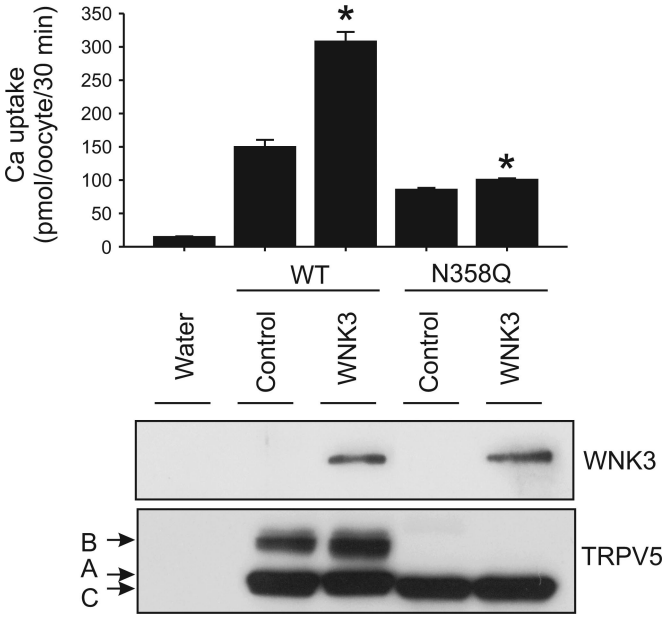

Fig. 4. Removal of *N*-linked glycosylation in TRPV5 blunted the effect of WNK3 on TRPV5. *Top*: WNK3 robustly increased Ca^{2+} influx mediated by wild-type TRPV5 (WT) but only modestly increased that of the N358Q mutant of TRPV5. *Bottom*: total protein level of WT and N358Q mutant of TRPV5 in the presence and absence of WNK3 revealed by Western blot analyses. Data from 3 batches of oocytes in each group are presented as means ± SE. *$P < 0.01$ vs. TRPV5 or N358Q alone group.

fully glycosylated protein will be inserted into the plasma membrane. The increase in the complexly glycosylated form of TRPV5 in the presence of WNK3 indicated that the delivery of TRPV5 along the secretory pathway to the plasma membrane was enhanced. We next disrupted the secretory pathway for TRPV5 insertion into the plasma membrane by removal of *N*-linked glycosylation in TRPV5. The N358Q mutation in the *N*-linked glycosylation site abolished the glycosylation of TRPV5, and only the unglycosylated form of TRPV5 (*band C*) was visible (Fig. 4, *bottom*). In this situation, the effect of WNK3 on TRPV5 was largely blunted (WNK3 increased wild-type by 105.7 ± 9.7% and N358Q by 17.6 ± 2.5%) (Fig. 4, *top*). This indicated that the major effect of WNK3 on TRPV5 resides in the secretory pathway of TRPV5 maturation and delivery to the plasma membrane.

We further measured the insertion of functional TRPV5 into the plasma membrane in a way similar to the approach used for measuring the rate of ENaC exocytosis (6). It has been reported that the thio reagent MTSET could irreversibly block rabbit TRPV5 and the cysteine 556 residue, which is likely located in the outer mouth of the channel pore and is responsible for the sensitivity of TRPV5 to MTSET (13). A serine residue is present at position 556 in human TRPV5, which was not blocked by MTSET (Fig. 5*A*). When serine 556 was mutated to a cysteine, the S556C mutant was blocked by MTSET by ~75%, as determined by measuring the Na^+ current (Fig. 5*B*). The ability of S556C to transport Ca^{2+} was not altered (Fig. 5*C*), and S556C was capable of being upregulated by WNK3 similarly to wild-type TRPV5 (Fig. 5*D*). To measure the insertion of functional TRPV5 into the plasma membrane, the oocytes expressing S556C mutant alone or with WNK3 were treated with 2 mM MTSET for 5 min, and then the recovery of S556C-mediated Na^+ current was determined at different time points. In the presence of WNK3, the rate of increase in S556C-mediated Na^+ current was significantly increased (Fig. 5*E*). Thus WNK3 may affect the maturation of TRPV5 and enhance the insertion of channels into the membrane from the subapical vesicle pools that contain "dormant" channels.

Since vesicular transport of secretory proteins is dependent on microtubules, we tested to what extent the effect of WNK3 on TRPV5 is sensitive to the microtubule inhibitor colchicine. Figure 6 indicated that the effect of WNK3 on TRPV5 was completely blocked by 2 mM colchicine, whereas 10 μM cytochalasin D, an inhibitor of actin microfilaments, was incapable of blocking the effect of WNK3 (Fig. 6, *top*). In fact, cytochalasin D slightly increased the TRPV5-mediated Ca^{2+} influx in both groups. The effectiveness of cytochalsin D was confirmed morphologically by the mottling of the pigments at the animal pole of the oocytes, and the effectiveness of colchicine was confirmed by the appearance of a pigment-free area in the topmost of the oocytes, which was caused by floating of the germinal vesicle due to the disruption of microtubes which support the germinal vesicle in the animal hemisphere (19) (Fig. 6, *bottom*). These effects were similar to those previously reported (10), although we observed that colchicine alone was sufficient to cause the drifting of the germinal vesicle.

WNK3 induced an increase in oocytes volume. It was noticed that the expression of WNK3 led the oocytes to swell. This situation worsened in the group coexpressed with WNK3 and TRPV5. These oocytes had a bulgy appearance 2 days after injection, and often a bubble formed in the site where a

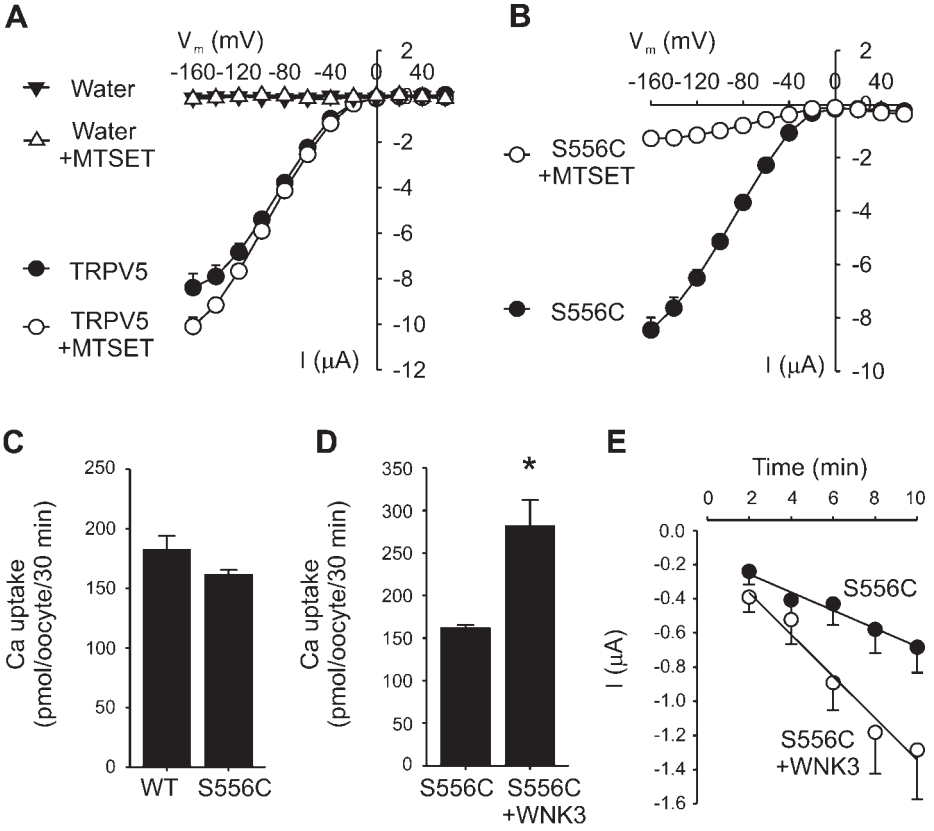

Fig. 5. WNK3 facilitated the delivery of new TRPV5 protein to the plasma membrane from its intracellular pool. *A*: Na^+-evoked current of wild-type human TRPV5 protein was not inhibited by 5 min treatment with 2 mM 2-trimethylammonium-ethyl-methanethiosulfonate bromide (MTSET). Data from 9 oocytes from 2 frogs in each group are presented as means ± SE. *B*: S556C mutant of TRPV5 was inhibited by 5-min treatment with 2 mM MTSET. Data from 20 oocytes from 2 frogs in each group are presented as means ± SE. *C*: TRPV5-mediated Ca^{2+} uptake was not significantly decreased by the S556C mutation. *D*: $^{45}Ca^{2+}$ uptake mediated by the S556C mutant was increased by WNK3. Data are presented as means ± SE of 3 independent experiments. *$P < 0.01$. *E*: rate of TRPV5 exocytosis was increased by WNK3. Shown are changes in TRPV5-mediated Na^+ currents (at −100 mV) at different time points after 5-min treatment with 2 mM MTSET. Data are presented as means ± SE from 9 oocytes in each group from 2 frogs.

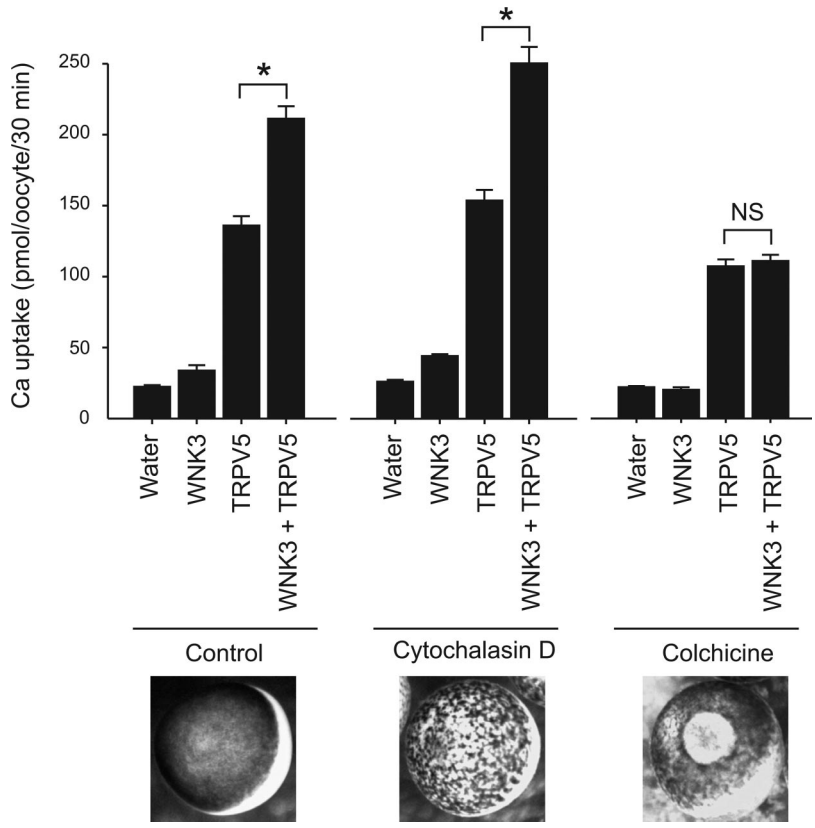

Fig. 6. Microtubule inhibitor colchicine blocked the effect of WNK3 on TRPV5. Oocytes were treated with 10 μM cytochalasin D, 2 mM colchicine, or vehicle (DMSO) right after injection, and $^{45}Ca^{2+}$ uptake experiments were performed 2 days after injection. Data are presented as means ± SE from 4 experiments. Representative pictures of oocytes treated with DMSO (control), cytochalasin D, and colchicine are shown (*bottom*). NS, not significantly different. *$P < 0.01$ vs. TRPV5 group.

glass needle was impaled during cRNA injection. To quantify this effect, we measured the oocyte diameter at *day 2* after injection and the corresponding oocyte volume and surface area were calculated (Fig. 7). A significant increase was observed in the group of oocytes expressing WNK3, and the increase was augmented when TRPV5 was coexpressed. The same was true for the groups expressing WNK4 alone or with TRPV5, albeit to a lesser extent. In the groups injected with WNK3 or WNK4, the cell surface area (cell volume) increased by 8.8 ± 0.8 (13.3 ± 1.3) and 4.1 ± 0.8 (6.1 ± 1.3%), respectively, over the water-injected control oocytes. When TRPV5 was coexpressed with WNK3 or WNK4, the cell surface area (cell volume) increased by 18.2 ± 0.7 (28.5 ± 1.2) and 9.2 ± 0.7 (14.1 ± 1.1%), respectively, over the TRPV5-injected group. The increase in Ca^{2+} uptake (Fig. 1*A*) was much higher than the increase in cell surface (Fig. 7); thus this increase in cell surface could not fully account for the increase in TRPV5-mediated Ca^{2+} transport.

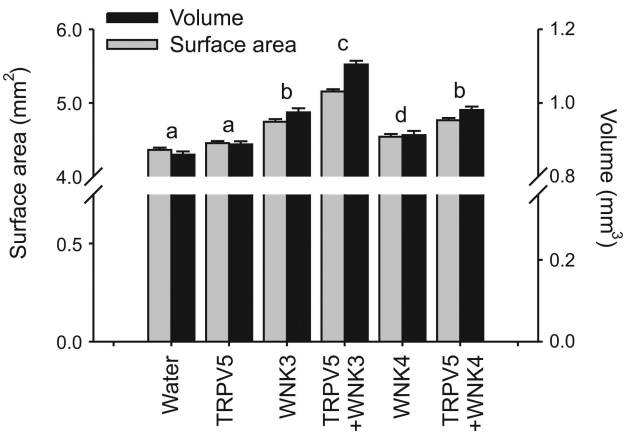

Fig. 7. Expression of WNK3 and WNK4 increased oocyte volume. Oocyte diameter was measured using a stereoscope equipped with a CCD camera. Over 50 oocytes from 5 batches of oocytes were measured at 2 days after injection. Both oocyte volume and surface area were calculated. Data are presented as means ± SE. Bars with the same superscript letters are not significantly different from one another ($P > 0.01$ by Student's *t*-test).

The kinase domain of WNK3 was necessary and sufficient for the enhancing effect on TRPV5. Mutation of a conserved aspartate residue at position 294 to alanine (D294A) was believed to abolish the kinase activity of WNK3 (30). D294A failed to increase TRPV5-mediated Ca^{2+} influx (Fig. 8*A*). On the contrary, a small inhibitory effect of the D294A mutant on TRPV5 was observed at 2 and 3 days after injection (Fig. 8*A*). This indicates that the kinase activity was necessary for the positive effect of WNK3. The effect of wild-type WNK3 on TRPV5 decreased at *day 3* after cRNA injection; however, we noticed that at *day 3* after injection, the oocytes expressing both WNK3 and TRPV5 deteriorated, likely due to the overexpression of TRPV5.

Full-length WNK3 constitutes the kinase domain in the NH_2-terminal region and the regulatory domain in the COOH-terminal region. To further clarify the roles of the kinase domain and the regulatory domain in the effect of WNK3 on TRPV5, we made two WNK3 constructs that contain the WNK3 NH_2-terminal kinase domain only (containing amino acids 1–413) or the WNK3 COOH-terminal regulatory domain only (containing amino acids 414–1800), respectively. With cRNA injection at the same molecule ratio, the WNK3 kinase domain was capable of increasing TRPV5-mediated Ca^{2+}

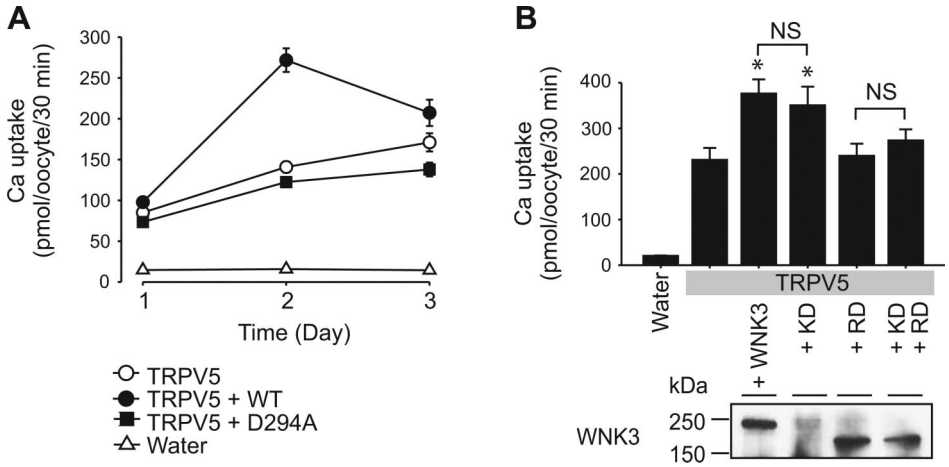

Fig. 8. Kinase activity of WNK3 was necessary and sufficient for its action on TRPV5. *A*: time-dependent effects of wild-type WNK3 (WT) and its kinase-inactivating D294A mutant on TRPV5. *X. laevis* oocytes were injected with water or 12.5 ng TRPV5 cRNA alone or together with WT WNK3 or D294A cRNA. Ca^{2+} uptake was assessed from 1 to 3 days after injection. Data are presented as means ± SE of 3 independent experiments. *B*: WNK3 kinase domain alone is capable of increasing TRPV5-mediated Ca^{2+} uptake. cRNAs of WNK3 kinase domain (KD; amino acids 1–413), regulatory domain (RD; amino acids 414–1800), and both KD and RD were coinjected into oocytes with TRPV5 cRNA. The KD and RD cRNA concentrations were adjusted so that equal number of RNA molecules for full-length WNK3, KD or RD was injected in respective groups. Ca^{2+} uptake was assessed 2 days after injection. Results are expressed as means ± SE of 3 independent experiments. $*P < 0.01$ vs. TRPV5 alone group; NS, not statistically different. *Bottom*: representative Western blot analysis of respective groups expressing WNK3 or its KD and RD. No specific signal was detected for the KD group because the WNK3 antibody recognized the COOH-terminal region of WNK3.

influx at a level not significantly different from full-length WNK3 (Fig. 8*B*). In contrast, the regulatory domain of WNK3 did not have any significant effect on TRPV5-mediated Ca^{2+} influx (Fig. 8*B*). Furthermore, the COOH-terminal regulatory domain appeared to block the effect of the kinase domain (Fig. 8*B*). This suggests that an inhibitory motif, which is not accessible in intact WNK3, might have been exposed in the artificially generated COOH-terminal regulatory domain. It is not clear whether this putative inhibitory motif is of physiological importance or is merely an artifact. The presence of full-length WNK3 and the regulatory domain of WNK3 was confirmed by Western blot analysis using a WNK3 antibody which recognizes the regulatory domain (Fig. 8*B*, *bottom*). These results demonstrated that the kinase domain of WNK3 was sufficient to increase TRPV5-mediated Ca^{2+} influx.

The important role of the kinase domain of WNK3 in the regulation of TRPV5 does not exclude the possibility that the regulatory domain of WNK3 also contributes to the regulation. In fact, most disease-causing mutations in WNK4 are located in an acidic motif outside the kinase domain (60). We constructed a FHH-like mutant WNK3 harboring a homologous mutation in this acidic region with the glutamine 545 residue substituted by a glutamate residue (Q545E; corresponding to FHH-causing WNK4 mutation Q565E). The Q545E mutant was modestly more potent than the wild-type WNK3 in increasing TRPV5-mediated Ca^{2+} uptake (Fig. 9). The expression level of wild-type and the Q545E mutant were comparable as determined by Western blot analysis (Fig. 9, *bottom*). Therefore, it appeared that the effect of WNK3 on TRPV5 could be modulated by the regulatory domain.

NCC partially blocked the positive effect of WNK3 on TRPV5. TRPV5 and NCC are coexpressed in the late segment of the DCT (35). The positive effect of WNK4 on TRPV5 is blocked by NCC in a dose-dependent manner (27). This observation was confirmed in current study (Fig. 10*A*). As shown in the Fig. 10*A*, the TRPV5-mediated Ca^{2+} influx was modestly decreased (by 17.9 ± 3.1%, $P < 0.01$) when NCC was coexpressed. In the presence of WNK3 and WNK4, NCC more robustly decreased TRPV5-mediated Ca^{2+} influx (by 28.9 ± 4.1 and 38.5 ± 3.3%, respectively) (Fig. 10*A*). In agreement with the Ca^{2+} influx data, the characteristic scarlike mark in oocytes expressing TRPV5 was also blocked by NCC (Fig. 10*B*).

WNK3 also exerted a positive effect on TRPV6. In contrast to the previous finding that WNK4 upregulated TRPV5 but not TRPV6, the TRPV6-mediated Ca^{2+} influx was increased by

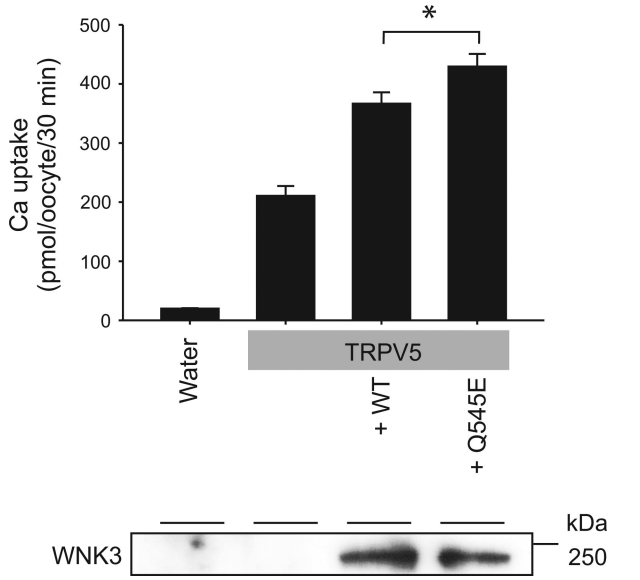

Fig. 9. Familial hyperkalemic hypertension (FHH)-like Q545E mutant of WNK3 exhibited increased ability to enhance TRPV5-mediated Ca^{2+} uptake compared with WT WNK3. Data from 3 independent experiments are expressed as means ± SE. $*P < 0.05$ by Student's *t*-test. *Bottom* :representative Western blot analysis with anti-WNK3 antibody.

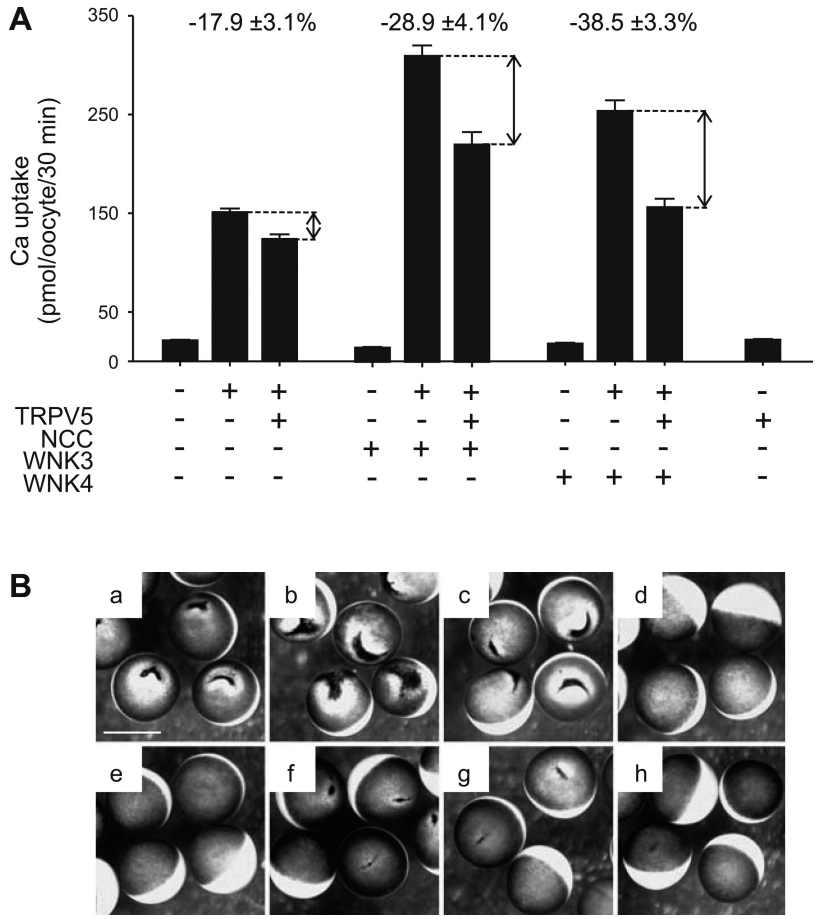

Fig. 10. Thiazide-sensitive Na-Cl cotransporter (NCC) partially blocked the effect of WNK3 on TRPV5. *A*: effect of NCC on TRPV5-mediated Ca^{2+} uptake in the presence or absence of WNK3 and WNK4. All Ca^{2+} uptake values from the groups coinjected with NCC were significantly ($P < 0.01$) lower than the corresponding groups without NCC. The percentage of inhibition is indicated above each set of results from each group. Data from 3 independent experiments are expressed as means ± SE. *B*: scale of the TRPV5 scarlike mark was significantly reduced by NCC. The characteristic TRPV5 scarlike marks formed in oocytes expressing TRPV5 (*a*), TRPV5 with WNK3 (*b*), or TRPV5 with WNK4 (*c*) were diminished in corresponding groups with NCC coexpressed (*e*, *f*, or *g*). Control water-injected oocytes (*d*) and NCC-expressing oocytes (*h*) didn't have scarlike marks. Bar = 1 mm.

65.8 ± 15.3% ($P < 0.01$) when WNK3 was coexpressed (Fig. 11*A*). In agreement with this observation, the Na^+ current of TRPV6 was also increased by WNK3 (Fig. 11*B*). The effect of WNK3 on TRPV6 appeared to be dependent on the catalytic activity of WNK3, as the kinase-inactive mutant D294A was incapable of increasing the TRPV6-mediated Ca^{2+} influx (Fig. 11*C*). The total TRPV6 protein level was increased by WNK3, as revealed by Western blot analysis using an antibody against TRPV6 (Fig. 11*D*). The total TRPV6 protein level in the presence of WNK3 was 170.0 ± 49.3% of that in the absence of WNK3, based on the intensity of all the TRPV6 bands from three independent experiments. These results suggested that WNK3 regulates TRPV5 and TRPV6 through a similar mechanism by increasing protein expression.

DISCUSSION

WNK3 was previously shown to be a potent regulator of SLC12A family members (12, 30, 47, 48), ROMK (34), and SLC26A9 (14). In the present study, we showed that WNK3 is also a positive regulator of the epithelial calcium channels TRPV5 and TRPV6. Furthermore, we showed that the kinase domain of WNK3 was sufficient to exert the positive effect on TRPV5. To our knowledge, this has not been observed for the WNK3-mediated regulation of other ion transport proteins. Since WNK3 is expressed in the distal tubule, where TRPV5 and TRPV6 are expressed, it might be a positive regulator of the active calcium reabsorption pathway in the kidney. In addition, as WNK3 is expressed in extrarenal tissues such as small intestine, stomach, and epididymis, where TRPV6 is expressed, the regulation of TRPV6 by WNK3 should bear physiological significance.

The antagonistic effect of WNK3 and WNK4 on NCC was not observed for TRPV5. This is likely due to the regulation of NCC by WNK3 and WNK4 through different mechanisms, whereas the actions of WNK3 and WNK4 on TRPV5 are through rather similar mechanisms, which are distinct from other regulatory mechanisms mediated by WNKs. In fact, the positive effect of WNK3 on TRPV5-mediated Ca^{2+} influx was more potent than that of WNK4, when the two kinases were tested side by side in the same batches of oocytes (Fig. 10). Both WNK3 (this study) and WNK4 (27) increased the surface level of TRPV5, and the complexly glycosylated form of TRPV5 was specifically increased. When the *N*-linked glycosylation of TRPV5 was abolished by mutagenesis, the enhancing effect of WNK3 was greatly reduced (Fig. 4). WNK3 appeared to be able to facilitate the core glycosylation of TRPV5 because the unglycosylated form of TRPV5 was decreased (Fig. 3*A*). Such an effect was not observed for WNK4 previously (27). Thus it is possible that WNK3 affects the protein processing in the endoplasmic reticulum, in addition to the maturation along the *trans*-Golgi network. TRPV6 reaches the plasma membrane mainly in core-glycosylated form in the *X. laevis* system (Jiang Y. et al., unpublished observations), whereas TRPV5 reaches the plasma membrane in a complexly glycosylated form (27). Unlike WNK3, WNK4 appears to be less capable of increasing the level of core-glycosylated TRPV5 or

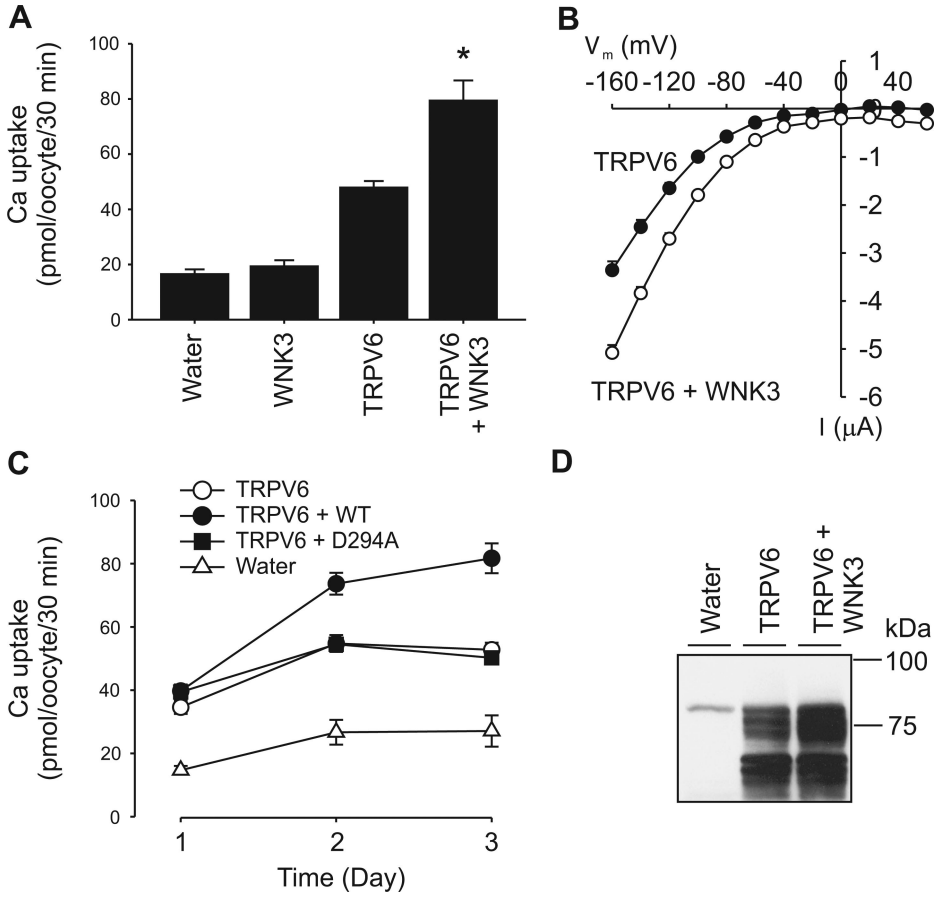

Fig. 11. Effects of WNK3 on TRPV6. *A*: TRPV6-mediated Ca^{2+} uptake was increased by WNK3. Data are presented as means ± SE of 3 independent experiments. *$P < 0.01$ vs. TRPV6 alone group. *B*: Na^+-evoked currents of TRPV6 were increased in the presence of WNK3. Shown are *I-V* plots of Na^+-evoked currents in oocytes expressing TRPV6 alone or with WNK3. Data are expressed as means ± SE from 22 oocytes from two frogs in each group. All experiments were performed at 2 days after injection of cRNAs. *C*: time dependence of WT WNK3 and its kinase-inactivating D294A mutant on TRPV6. *X. laevis* oocytes were injected with water or 12.5 ng TRPV6 cRNA alone or together with 12.5 ng WT WNK3 or D294A cRNA. Ca^{2+} uptake was assessed from 1 to 3 days after injection. Data are presented as means ± SE of 3 independent experiments. *D*: protein level of TRPV6 was increased by WNK3. Shown is a representative Western blot analysis using antibody against TRPV6.

TPRV6. This may explain why WNK4 only enhances TRPV5, whereas WNK3 enhances both TRPV5 and TRPV6. WNK4 was postulated to inhibit the forward trafficking of NCC (5, 21); however, both WNK3 and WNK4 appear to enhance the forward trafficking of TRPV5. How a protein affects the same pathway in different directions on different transporters remains elusive.

It has been shown that WNK3 is capable of regulating different ion transport proteins via kinase-dependent or kinase-independent mechanisms. WNK3 increases Na-K-2Cl cotransporter NKCC1 activity and inhibits K-Cl cotransporters KCC1 and KCC2, bypassing the normal requirement of altered tonicity for activation of these transporters through a mechanism that involves phosphorylation of NKCC1 (30). Similarly, wild-type WNK3 increases NCC and NKCC2, which are expressed in the DCT and thick ascending limb (48). The kinase-inactive mutant of WNK3 acts in the opposite direction compared with wild-type WNK3 (30, 48). WNK3 prevents the swelling-induced activation of KCC1 to KCC4; and the kinase-inactive D294A mutant abolished the cell shrinkage-induced inhibition of KCC1 to KCC4 via a phosphatase-dependent pathway (12). This regulation of KCC4 could not be achieved with the D294A kinase domain or the regulatory domain, or both, suggesting that the kinase-inactive WNK3 may interact with both KCC4 and the phosphatase using different domains (12). The above regulation of SLC12A family members by WNK3 appears to involve the kinase activity of WNK3. However, although NCC is inhibited by a kinase-inactive mutant of WNK3, the COOH terminus of WNK3 (421–1743) is as effective as wild-type WNK3 in stimulating NCC (68), in a way similar to the WNK4-mediated regulation of NCC (69). In contrast, ROMK and SLC26A9 are inhibited by WNK3 in a kinase independent manner (14, 34). The kinase-inactive mutant of WNK3 exhibited a more potent inhibitory effect on ROMK than wild-type WNK3. Furthermore, the regulatory domain of WNK3 is capable of inhibiting ROMK. Similarly, the Cl^- channel SLC26A9 is regulated by WNK3 in a kinase-independent fashion (14). The kinase-inactive K159M mutant of WNK3 is capable of inhibiting SLC26A9 as is wild-type WNK3, and the kinase domain of WNK3 (amino acids 1–410) is unable to inhibit SLC26A9. Thus ROMK and SLC26A9 are two channels under the inhibitory regulation of WNK3 in a kinase-independent manner.

The WNK3-mediated regulation of TRPV5 appeared different from what has been described for other ion transport proteins. In contrast, WNK3 acted similarly to WNK4 on the regulation of TRPV5. We previously showed that only kinase-intact WNK4 was capable of increasing TRPV5 (27). The same is true for the regulation of TRPV5 and TRPV6 by WNK3. In fact, the kinase domain of WNK3 alone was sufficient in enhancing the TRPV5-mediated Ca^{2+} influx. To our knowledge, this is the first example that the kinase domain of WNK3 alone is capable of mediating positive regulation of a transporter or ion channel. Since the major effect of WNK3 on TRPV5 is to increase the matured channel proteins at the plasma membrane, it is likely that the kinase activity of WNK3 is important to regulate the protein maturation and insertion into the plasma membrane along the secretory pathway. Al-

though whether WNK3 regulates the phosphorylation of TRPV5 (or TRPV6) is yet to be determined, it is more likely that WNK3 acts on its targets involved in steps of protein processing and maturation, such as key proteins in the secretory pathway, rather than TRPV5 itself. TPRV5 and TRPV6 are examples of the proteins that are affected by these steps. Thus phosphorylation of TRPV5 or TRPV6 directly by WNK3 is possible, but this is not necessary to explain the actions of WNK3 on these proteins. It is worth noting that the fact that WNK3 affects the secretory pathway does not exclude the possibility that it also has an effect on TRPV5/TRPV6 internalization, which is yet to be examined.

An interesting observation in this study is that the oocytes expressing exogenous WNK3 swelled in the culture. The same occurred in oocytes expressing WNK4, but to a much lesser extent. Oocyte swelling is due to the increased ion and water influx, indicating that endogenous ion- and water-transporting proteins were regulated. It has been shown that WNK3 regulates SLC12A family members, which are involved in cell volume regulation (12, 30, 47, 48). For example, the entry pathways of Cl^- into the oocytes were activated, and the exit pathways of Cl^- were blocked by WNK3. This will cause an increase in Cl^- concentration, which will in turn cause water to enter passively to maintain the balanced osmolarity inside the oocyte. This regulation will result in oocyte volume expansion. It is possible that similar endogenous proteins in *X. laevis* oocytes were regulated by WNK3, possibly via pathways similar to what we observed for TRPV5 or pathways as previously described (12, 14, 30, 34, 48).

We previously demonstrated that the thiazide-sensitive Na-Cl cotransporter NCC blocked the effect of WNK4 (27). In the present study, we showed that the effect of WNK3 on TRPV5 could be attenuated by NCC as well. It was recently shown that WNK3 interacts with WNK4 and is likely a part of the WNK signaling complex (68). As WNK3, WNK4, and NCC are coexpressed with TRPV5 in the DCT, the positive effects of WNK3 and WNK4 on TRPV5 are likely modulated by NCC. As NCC is enhanced by WNK3 (48, 68) and is decreased by WNK4 (61, 67), both WNK3 and WNK4 increase TRPV5 (27), and NCC blocks both effects of WNK3 and WNK4 on TRPV5 (27), the overall effect of these regulations on TRPV5 likely depends on the relative levels of NCC and the WNKs.

In summary, we demonstrated that WNK3 increased Ca^{2+} influx mediated by TRPV5 (and also TRPV6) through enhancing the membrane expression level of the functional channel proteins via a kinase-dependent pathway. The mechanisms of regulation of TRPV5 by WNK3 and WNK4 are, at least in part, in the maturation and delivery of TRPV5 to the plasma membrane via the secretory pathway. The actions of WNK3 and WNK4 on other ion transport proteins taken into account, WNK3 and WNK4 are remarkable, multiple-function regulators which have different actions on different ion transport pathways. The specificity of the regulation of a peculiar ion transport protein by these WNKs likely resides in the ion transport protein itself, e.g., whether the protein is regulated via a pathway affected by the WNKs.

ACKNOWLEDGMENTS

The authors thank Drs. Xavier Jeunemaitre and Juliette Hadchouel for WNK4 cDNA. Part of this work was presented as an abstract at Experimental Biology 2008, San Diego, CA, April 5–9, 2008.

GRANTS

This work was supported by National Institute of Diabetes and Digestive and Kidney Diseases Grant R01-DK-072154.

REFERENCES

1. **Achard JM, Warnock DG, Disse-Nicodeme S, Fiquet-Kempf BB, Corvol P, Fournier A, Jeunemaitre X.** Familial hyperkalemic hypertension: phenotypic analysis in a large family with the WNK1 deletion mutation. *Am J Med* 114: 495–498, 2003.
2. **Anselmo AN, Earnest S, Chen W, Juang YC, Kim SC, Zhao Y, Cobb MH.** WNK1 and OSR1 regulate the Na^+, K^+, $2Cl^-$ cotransporter in HeLa cells. *Proc Natl Acad Sci USA* 103: 10883–10888, 2006.
3. **Bianco SD, Peng JB, Takanaga H, Suzuki Y, Crescenzi A, Kos CH, Zhuang L, Freeman MR, Gouveia CH, Wu J, Luo H, Mauro T, Brown EM, Hediger MA.** Marked disturbance of calcium homeostasis in mice with targeted disruption of the Trpv6 calcium channel gene. *J Bone Miner Res* 22: 274–285, 2007.
4. **Bohmer C, Palmada M, Kenngott C, Lindner R, Klaus F, Laufer J, Lang F.** Regulation of the epithelial calcium channel TRPV6 by the serum and glucocorticoid-inducible kinase isoforms SGK1 and SGK3. *FEBS Lett* 581: 5586–5590, 2007.
5. **Cai H, Cebotaru V, Wang YH, Zhang XM, Cebotaru L, Guggino SE, Guggino WB.** WNK4 kinase regulates surface expression of the human sodium chloride cotransporter in mammalian cells. *Kidney Int* 69: 2162–2170, 2006.
6. **Carattino MD, Hill WG, Kleyman TR.** Arachidonic acid regulates surface expression of epithelial sodium channels. *J Biol Chem* 278: 36202–36213, 2003.
7. **Cha SK, Ortega B, Kurosu H, Rosenblatt KP, Kuro O, Huang CL.** Removal of sialic acid involving Klotho causes cell-surface retention of TRPV5 channel via binding to galectin-1. *Proc Natl Acad Sci USA* 105: 9805–9810, 2008.
8. **Cha SK, Wu T, Huang CL.** Protein kinase C inhibits caveolae-mediated endocytosis of TRPV5. *Am J Physiol Renal Physiol* 294: F1212–F1221, 2008.
9. **Chang Q, Hoefs S, van der Kemp AW, Topala CN, Bindels RJ, Hoenderop JG.** The beta-glucuronidase klotho hydrolyzes and activates the TRPV5 channel. *Science* 310: 490–493, 2005.
10. **Colman A, Morser J, Lane C, Besley J, Wylie C, Valle G.** Fate of secretory proteins trapped in oocytes of *Xenopus laevis* by disruption of the cytoskeleton or by imbalanced subunit synthesis. *J Cell Biol* 91: 770–780, 1981.
11. **Cope G, Murthy M, Golbang AP, Hamad A, Liu CH, Cuthbert AW, O'shaughnessy KM.** WNK1 affects surface expression of the ROMK potassium channel independent of WNK4. *J Am Soc Nephrol* 17: 1867–1874, 2006.
12. **de Los Heros P, Kahle KT, Rinehart J, Bobadilla NA, Vazquez N, San CP, Mount DB, Lifton RP, Hebert SC, Gamba G.** WNK3 bypasses the tonicity requirement for K-Cl cotransporter activation via a phosphatase-dependent pathway. *Proc Natl Acad Sci USA* 103: 1976–1981, 2006.
13. **Dodier Y, Banderali U, Klein H, Topalak O, Dafi O, Simoes M, Bernatchez G, Sauve R, Parent L.** Outer pore topology of the ECaC-TRPV5 channel by cysteine scan mutagenesis. *J Biol Chem* 279: 6853–6862, 2004.
14. **Dorwart MR, Shcheynikov N, Wang Y, Stippec S, Muallem S.** SLC26A9 is a Cl^- channel regulated by the WNK kinases. *J Physiol* 584: 333–345, 2007.
15. **Embark HM, Setiawan I, Poppendieck S, van de Graaf SF, Boehmer C, Palmada M, Wieder T, Gerstberger R, Cohen P, Yun CC, Bindels RJ, Lang F.** Regulation of the epithelial Ca^{2+} channel TRPV5 by the NHE regulating factor NHERF2 and the serum and glucocorticoid inducible kinase isoforms SGK1 and SGK3 expressed in *Xenopus* oocytes. *Cell Physiol Biochem* 14: 203–212, 2004.
16. **Farfel Z, Mayan H, Yaacov Y, Mouallem M, Shaharabany M, Pauzner R, Kerem E, Wilschanski M.** WNK4 regulates airway Na^+ transport: study of familial hyperkalaemia and hypertension. *Eur J Clin Invest* 35: 410–415, 2005.

17. **Fu Y, Subramanya A, Rozansky D, Cohen DM.** WNK kinases influence TRPV4 channel function and localization. *Am J Physiol Renal Physiol* 290: F1305–F1314, 2006.
18. **Gagnon KB, England R, Delpire E.** Volume sensitivity of cation-Cl^- cotransporters is modulated by the interaction of two kinases: Ste20-related proline-alanine-rich kinase and WNK4. *Am J Physiol Cell Physiol* 290: C134–C142, 2006.
19. **Gard DL.** Organization, nucleation, and acetylation of microtubules in *Xenopus laevis* oocytes: a study by confocal immunofluorescence microscopy. *Dev Biol* 143: 346–362, 1991.
20. **Garzon-Muvdi T, Pacheco-Alvarez D, Gagnon KB, Vazquez N, Ponce-Coria J, Moreno E, Delpire E, Gamba G.** WNK4 kinase is a negative regulator of K^+-Cl^- cotransporters. *Am J Physiol Renal Physiol* 292: F1197–F1207, 2007.
21. **Golbang AP, Cope G, Hamad A, Murthy M, Liu CH, Cuthbert AW, O'shaughnessy KM.** Regulation of the expression of the Na/Cl cotransporter by WNK4 and WNK1: evidence that accelerated dynamin-dependent endocytosis is not involved. *Am J Physiol Renal Physiol* 291: F1369–F1376, 2006.
22. **Golbang AP, Murthy M, Hamad A, Liu CH, Cope G, Van't HW, Cuthbert A, O'shaughnessy KM.** A new kindred with pseudohypoaldosteronism type II and a novel mutation (564D>H) in the acidic motif of the WNK4 gene. *Hypertension* 46: 295–300, 2005.
23. **Hadchouel J, Delaloy C, Faure S, Achard JM, Jeunemaitre X.** Familial hyperkalemic hypertension. *J Am Soc Nephrol* 17: 208–217, 2006.
24. **He G, Wang HR, Huang SK, Huang CL.** Intersectin links WNK kinases to endocytosis of ROMK1. *J Clin Invest* 117: 1078–1087, 2007.
25. **Hoenderop JG, van der Kemp AW, Hartog A, van de Graaf SF, Van Os CH, Willems PH, Bindels RJ.** Molecular identification of the apical Ca^{2+} channel in 1,25-dihydroxyvitamin D_3-responsive epithelia. *J Biol Chem* 274: 8375–8378, 1999.
26. **Hoenderop JG, van Leeuwen JP, van der Eerden BC, Kersten FF, van der Kemp AW, Merillat AM, Waarsing JH, Rossier BC, Vallon V, Hummler E, Bindels RJ.** Renal Ca^{2+} wasting, hyperabsorption, and reduced bone thickness in mice lacking TRPV5. *J Clin Invest* 112: 1906–1914, 2003.
27. **Jiang Y, Ferguson WB, Peng JB.** WNK4 enhances TRPV5-mediated calcium transport: potential role in hypercalciuria of familial hyperkalemic hypertension caused by gene mutation of WNK4. *Am J Physiol Renal Physiol* 292: F545–F554, 2007.
28. **Kahle KT, Gimenez I, Hassan H, Wilson FH, Wong RD, Forbush B, Aronson PS, Lifton RP.** WNK4 regulates apical and basolateral Cl^- flux in extrarenal epithelia. *Proc Natl Acad Sci USA* 101: 2064–2069, 2004.
29. **Kahle KT, MacGregor GG, Wilson FH, Van Hoek AN, Brown D, Ardito T, Kashgarian M, Giebisch G, Hebert SC, Boulpaep EL, Lifton RP.** Paracellular Cl^- permeability is regulated by WNK4 kinase: insight into normal physiology and hypertension. *Proc Natl Acad Sci USA* 101: 14877–14882, 2004.
30. **Kahle KT, Rinehart J, de los HP, Louvi A, Meade P, Vazquez N, Hebert SC, Gamba G, Gimenez I, Lifton RP.** WNK3 modulates transport of Cl^- in and out of cells: implications for control of cell volume and neuronal excitability. *Proc Natl Acad Sci USA* 102: 16783–16788, 2005.
31. **Kahle KT, Wilson FH, Leng Q, Lalioti MD, O'Connell AD, Dong K, Rapson AK, MacGregor GG, Giebisch G, Hebert SC, Lifton RP.** WNK4 regulates the balance between renal NaCl reabsorption and K^+ secretion. *Nat Genet* 35: 372–376, 2003.
32. **Lalioti MD, Zhang J, Volkman HM, Kahle KT, Hoffmann KE, Toka HR, Nelson-Williams C, Ellison DH, Flavell R, Booth CJ, Lu Y, Geller DS, Lifton RP.** Wnk4 controls blood pressure and potassium homeostasis via regulation of mass and activity of the distal convoluted tubule. *Nat Genet* 38: 1124–1132, 2006.
33. **Lazrak A, Liu Z, Huang CL.** Antagonistic regulation of ROMK by long and kidney-specific WNK1 isoforms. *Proc Natl Acad Sci USA* 103: 1615–1620, 2006.
34. **Leng Q, Kahle KT, Rinehart J, MacGregor GG, Wilson FH, Canessa CM, Lifton RP, Hebert SC.** WNK3, a kinase related to genes mutated in hereditary hypertension with hyperkalaemia, regulates the K^+ channel ROMK1 (Kir1.1). *J Physiol* 571: 275–286, 2006.
35. **Loffing J, Loffing-Cueni D, Valderrabano V, Klausli L, Hebert SC, Rossier BC, Hoenderop JG, Bindels RJ, Kaissling B.** Distribution of transcellular calcium and sodium transport pathways along mouse distal nephron. *Am J Physiol Renal Physiol* 281: F1021–F1027, 2001.
36. **Maley F, Trimble RB, Tarentino AL, Plummer TH Jr.** Characterization of glycoproteins and their associated oligosaccharides through the use of endoglycosidases. *Anal Biochem* 180: 195–204, 1989.
37. **Mayan H, Munter G, Shaharabany M, Mouallem M, Pauzner R, Holtzman EJ, Farfel Z.** Hypercalciuria in familial hyperkalemia and hypertension accompanies hyperkalemia and precedes hypertension: description of a large family with the Q565E WNK4 mutation. *J Clin Endocrinol Metab* 89: 4025–4030, 2004.
38. **Mayan H, Vered I, Mouallem M, Tzadok-Witkon M, Pauzner R, Farfel Z.** Pseudohypoaldosteronism type II: marked sensitivity to thiazides, hypercalciuria, normomagnesemia, and low bone mineral density. *J Clin Endocrinol Metab* 87: 3248–3254, 2002.
39. **Min X, Lee BH, Cobb MH, Goldsmith EJ.** Crystal structure of the kinase domain of WNK1, a kinase that causes a hereditary form of hypertension. *Structure* 12: 1303–1311, 2004.
40. **Moriguchi T, Urushiyama S, Hisamoto N, Iemura S, Uchida S, Natsume T, Matsumoto K, Shibuya H.** WNK1 regulates phosphorylation of cation-chloride-coupled cotransporters via the STE20-related kinases, SPAK and OSR1. *J Biol Chem* 280: 42685–42693, 2005.
41. **Naray-Fejes-Toth A, Snyder PM, Fejes-Toth G.** The kidney-specific WNK1 isoform is induced by aldosterone and stimulates epithelial sodium channel-mediated Na^+ transport. *Proc Natl Acad Sci USA* 101: 17434–17439, 2004.
42. **Ohta A, Yang SS, Rai T, Chiga M, Sasaki S, Uchida S.** Overexpression of human WNK1 increases paracellular chloride permeability and phosphorylation of claudin-4 in MDCKII cells. *Biochem Biophys Res Commun* 349: 804–808, 2006.
43. **Palmada M, Poppendieck S, Embark HM, van de Graaf SF, Boehmer C, Bindels RJ, Lang F.** Requirement of PDZ domains for the stimulation of the epithelial Ca^{2+} channel TRPV5 by the NHE regulating factor NHERF2 and the serum and glucocorticoid inducible kinase SGK1. *Cell Physiol Biochem* 15: 175–182, 2005.
44. **Peng JB, Brown EM, Hediger MA.** Structural conservation of the genes encoding CaT1, CaT2, and related cation channels. *Genomics* 76: 99–109, 2001.
45. **Peng JB, Chen XZ, Berger UV, Vassilev PM, Tsukaguchi H, Brown EM, Hediger MA.** Molecular cloning and characterization of a channel-like transporter mediating intestinal calcium absorption. *J Biol Chem* 274: 22739–22746, 1999.
46. **Peng JB, Chen XZ, Berger UV, Weremowicz S, Morton CC, Vassilev PM, Brown EM, Hediger MA.** Human calcium transport protein CaT1. *Biochem Biophys Res Commun* 278: 326–332, 2000.
47. **Ponce-Coria J, San-Cristobal P, Kahle KT, Vazquez N, Pacheco-Alvarez D, de los HP, Juarez P, Munoz E, Michel G, Bobadilla NA, Gimenez I, Lifton RP, Hebert SC, Gamba G.** Regulation of NKCC2 by a chloride-sensing mechanism involving the WNK3 and SPAK kinases. *Proc Natl Acad Sci USA* 105: 8458–8463, 2008.
48. **Rinehart J, Kahle KT, de los HP, Vazquez N, Meade P, Wilson FH, Hebert SC, Gimenez I, Gamba G, Lifton RP.** WNK3 kinase is a positive regulator of NKCC2 and NCC, renal cation-Cl^- cotransporters required for normal blood pressure homeostasis. *Proc Natl Acad Sci USA* 102: 16777–16782, 2005.
49. **Ring AM, Cheng SX, Leng Q, Kahle KT, Rinehart J, Lalioti MD, Volkman HM, Wilson FH, Hebert SC, Lifton RP.** WNK4 regulates activity of the epithelial Na^+ channel in vitro and in vivo. *Proc Natl Acad Sci USA* 104: 4020–4024, 2007.
50. **Ring AM, Leng Q, Rinehart J, Wilson FH, Kahle KT, Hebert SC, Lifton RP.** An SGK1 site in WNK4 regulates Na^+ channel and K^+ channel activity and has implications for aldosterone signaling and K^+ homeostasis. *Proc Natl Acad Sci USA* 104: 4025–4029, 2007.
51. **Song Y, Peng X, Porta A, Takanaga H, Peng JB, Hediger MA, Fleet JC, Christakos S.** Calcium transporter 1 and epithelial calcium channel messenger ribonucleic acid are differentially regulated by 1,25 dihydroxyvitamin D_3 in the intestine and kidney of mice. *Endocrinology* 144: 3885–3894, 2003.
52. **Suzuki Y, Kovacs CS, Takanaga H, Peng JB, Landowski CP, Hediger MA.** Calcium channel TRPV6 is involved in murine maternal-fetal calcium transport. *J Bone Miner Res* 23: 1249–1256, 2008.
53. **Van Cromphaut SJ, Dewerchin M, Hoenderop JG, Stockmans I, Van Herck E, Kato S, Bindels RJ, Collen D, Carmeliet P, Bouillon R, Carmeliet G.** Duodenal calcium absorption in vitamin D receptor-knockout mice: functional and molecular aspects. *Proc Natl Acad Sci USA* 98: 13324–13329, 2001.

54. **Van Cromphaut SJ, Rummens K, Stockmans I, Van Herck E, Dijcks FA, Ederveen AG, Carmeliet P, Verhaeghe J, Bouillon R, Carmeliet G.** Intestinal calcium transporter genes are upregulated by estrogens and the reproductive cycle through vitamin D receptor-independent mechanisms. *J Bone Miner Res* 18: 1725–1736, 2003.
55. **van de Graaf SF, Hoenderop JG, Gkika D, Lamers D, Prenen J, Rescher U, Gerke V, Staub O, Nilius B, Bindels RJ.** Functional expression of the epithelial Ca^{2+} channels (TRPV5 and TRPV6) requires association of the S100A10-annexin 2 complex. *EMBO J* 22: 1478–1487, 2003.
56. **Verissimo F, Jordan P.** WNK kinases, a novel protein kinase subfamily in multi-cellular organisms. *Oncogene* 20: 5562–5569, 2001.
57. **Vitari AC, Deak M, Morrice NA, Alessi DR.** The WNK1 and WNK4 protein kinases that are mutated in Gordon's hypertension syndrome phosphorylate and activate SPAK and OSR1 protein kinases. *Biochem J* 391: 17–24, 2005.
58. **Vitari AC, Thastrup J, Rafiqi FH, Deak M, Morrice NA, Karlsson HK, Alessi DR.** Functional interactions of the SPAK/OSR1 kinases with their upstream activator WNK1 and downstream substrate NKCC1. *Biochem J* 397: 223–231, 2006.
59. **Wade JB, Fang L, Liu J, Li D, Yang CL, Subramanya AR, Maouyo D, Mason A, Ellison DH, Welling PA.** WNK1 kinase isoform switch regulates renal potassium excretion. *Proc Natl Acad Sci USA* 103: 8558–8563, 2006.
60. **Wilson FH, Disse-Nicodeme S, Choate KA, Ishikawa K, Nelson-Williams C, Desitter I, Gunel M, Milford DV, Lipkin GW, Achard JM, Feely MP, Dussol B, Berland Y, Unwin RJ, Mayan H, Simon DB, Farfel Z, Jeunemaitre X, Lifton RP.** Human hypertension caused by mutations in WNK kinases. *Science* 293: 1107–1112, 2001.
61. **Wilson FH, Kahle KT, Sabath E, Lalioti MD, Rapson AK, Hoover RS, Hebert SC, Gamba G, Lifton RP.** Molecular pathogenesis of inherited hypertension with hyperkalemia: the Na-Cl cotransporter is inhibited by wild-type but not mutant WNK4. *Proc Natl Acad Sci USA* 100: 680–684, 2003.
62. **Wood RJ, Tchack L, Taparia S.** 1,25-Dihydroxyvitamin D_3 increases the expression of the CaT1 epithelial calcium channel in the Caco-2 human intestinal cell line. *BMC Physiol* 1: 11, 2001.
63. **Xu B, English JM, Wilsbacher JL, Stippec S, Goldsmith EJ, Cobb MH.** WNK1, a novel mammalian serine/threonine protein kinase lacking the catalytic lysine in subdomain II. *J Biol Chem* 275: 16795–16801, 2000.
64. **Xu BE, Stippec S, Chu PY, Lazrak A, Li XJ, Lee BH, English JM, Ortega B, Huang CL, Cobb MH.** WNK1 activates SGK1 to regulate the epithelial sodium channel. *Proc Natl Acad Sci USA* 102: 10315–10320, 2005.
65. **Xu BE, Stippec S, Lazrak A, Huang CL, Cobb MH.** WNK1 activates SGK1 by a phosphatidylinositol 3-kinase-dependent and non-catalytic mechanism. *J Biol Chem* 280: 34218–34223, 2005.
66. **Yamauchi K, Rai T, Kobayashi K, Sohara E, Suzuki T, Itoh T, Suda S, Hayama A, Sasaki S, Uchida S.** Disease-causing mutant WNK4 increases paracellular chloride permeability and phosphorylates claudins. *Proc Natl Acad Sci USA* 101: 4690–4694, 2004.
67. **Yang CL, Angell J, Mitchell R, Ellison DH.** WNK kinases regulate thiazide-sensitive Na-Cl cotransport. *J Clin Invest* 111: 1039–1045, 2003.
68. **Yang CL, Zhu X, Ellison DH.** The thiazide-sensitive Na-Cl cotransporter is regulated by a WNK kinase signaling complex. *J Clin Invest* 117: 3403–3411, 2007.
69. **Yang CL, Zhu X, Wang Z, Subramanya AR, Ellison DH.** Mechanisms of WNK1 and WNK4 interaction in the regulation of thiazide-sensitive NaCl cotransport. *J Clin Invest* 115: 1379–1387, 2005.
70. **Yang SS, Morimoto T, Rai T, Chiga M, Sohara E, Ohno M, Uchida K, Lin SH, Moriguchi T, Shibuya H, Kondo Y, Sasaki S, Uchida S.** Molecular pathogenesis of pseudohypoaldosteronism type II: generation and analysis of a Wnk4(D561A/+) knockin mouse model. *Cell Metab* 5: 331–344, 2007.
71. **Zhuang L, Peng JB, Tou L, Takanaga H, Adam RM, Hediger MA, Freeman MR.** Calcium-selective ion channel, CaT1, is apically localized in gastrointestinal tract epithelia and is aberrantly expressed in human malignancies. *Lab Invest* 82: 1755–1764, 2002.